Examining the Chirality, Conformation and Selective Kinase Inhibition of 3-((3*R*,4*R*)-4-methyl-3-(methyl(7H-pyrrolo[2,3-*d*]pyrimidin-4-yl)amino)piperidin-1-yl)-3-oxopropanenitrile (CP-690,550)

Jian-kang Jiang,[†] Kamran Ghoreschi,[‡] Francesca Deflorian,[§] Zhi Chen,[‡] Melissa Perreira,[†] Marko Pesu,[‡] Jeremy Smith,[⊥] Dac-Trung Nguyen,[†] Eric H. Liu,[∥] William Leister,[†] Stefano Costanzi,[§] John J. O'Shea,[‡] and Craig J. Thomas*[,†]

NIH Chemical Genomics Center, National Human Genome Research Institute, National Institutes of Health, 9800 Medical Center Drive, Rockville, Maryland 20850, Molecular Immunology and Inflammation Branch, National Institute of Arthritis and Musculoskelatal and Skin Diseases, National Institutes of Health, Bethesda, Maryland 20850, Laboratory of Biological Modeling and Transplantation and Autoimmunity Branch, National Institute of Diabetes and Digestive and Kidney Diseases, National Institutes of Health, Bethesda, Maryland 20892, Kelly Services, 6101 Executive Boulevard, Room 392, Mail Stop Code 9307, Rockville, Maryland 20852

Received September 12, 2008

Here, we examine the significance that stereochemistry plays within the clinically relevant Janus kinase 3 (Jak3) inhibitor **1** (CP-690,550). A synthesis of all four enantiopure stereoisomers of the drug was carried out and an examination of each compound revealed that only the enantiopure 3*R*,4*R* isomer was capable of blocking Stat5 phosphorylation (Jak3 dependent). Each compound was profiled across a panel of over 350 kinases, which revealed a high level of selectivity for the Jak family kinases for these related compounds. Each stereoisomer retained a degree of binding to Jak3 and Jak2 and the 3*R*,4*S* and 3*S*,4*R* stereoisomers were further revealed to have binding affinity for selected members of the STE7 and STE20 subfamily of kinases. Finally, an appraisal of the minimum energy conformation of each stereoisomer and molecular docking at Jak3 was performed in an effort to better understand each compounds selectivity and potency profiles.

Introduction

The potent and selective Janus kinase 3 (Jak3[a]) inhibitor 3-((3*R*,4*R*)-4-methyl-3-(methyl(7*H*-pyrrolo[2,3-*d*]pyrimidin-4-yl)amino)piperidin-1-yl)-3-oxopropanenitrile (**1**) (CP-690,550) was reported in 2003 as an orally active immunosuppressant for autoimmune disease and transplant patients.[1] The structure was revealed as a substituted piperidine linked to a deazapurine core (**1**) (Figure 1). Interestingly, the initial report did not designate the stereochemistry at the 3 and 4 positions of the substituted piperidine ring. Reports within the patent literature[2−4] and subsequent manuscripts[5,6] have denoted the structure as the enantiopure (3*R*,4*R*) analogue **1**. At the time of writing, **1** has demonstrated efficacy in phase 2 clinical evaluation as an immunosuppressive for renal transplant rejection[7] and for treatment of rheumatoid arthritis.[8] Undoubtedly, a major foundation for the clinical success of this agent is the potent and selective Jak3 inhibition. The original report provided evidence that **1** inhibited Jak3 with an IC_{50} value of 1 nM while inhibiting Jak2, Jak1, Rock-II, and Lck with IC_{50} values of 20, 112, 3400, and 3870 nM, respectively.[1] A panel of 28 other kinases did not demonstrate any relevant inhibition. Recently, Karaman et al. presented the interaction maps for 38 clinically relevant kinase inhibitors across a panel of 317 kinases.[9] The manuscript included **1** and reported the binding potential at Jak3 and Jak2 as 2.2 and 5 nM (K_d) [the primary kinase domain of Jak1 was not incorporated in this screen], respectively. The report included additional binding for **1** at Camk1 (K_d of 5000 nM), DCamkL3 (K_d of 4.5 nM), Mst2 (K_d of 4300 nM), Pkn1 (K_d of 200 nM), Rps6ka2 (Kin.Dom.2−C-terminal) (K_d of 1400 nM), Rps6ka6 (Kin.Dom.2−C-terminal) (K_d of 1200 nM), Snark (K_d of 420 nM), Tnk1 (K_d of 640 nM), and Tyk2 (K_d of 620 nM).

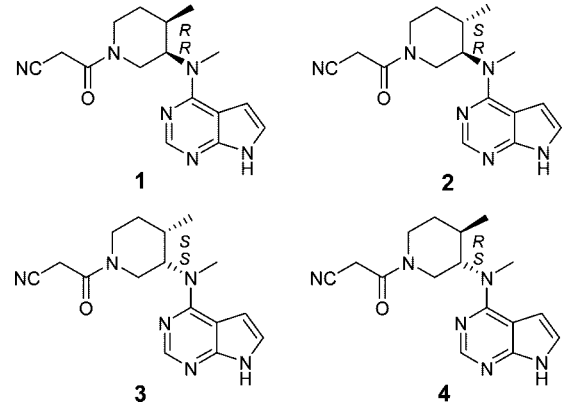

Figure 1. The chemical structure of **1** and related stereoisomers **2**, **3**, and **4**.

Despite these additional activities, **1** remains a remarkably selective kinase inhibitor. In a recent report, Changelian et al. related the clinical success of Jak3 inhibitors directly to their selectivity.[10] As the binding of any small molecule to a protein target is inextricably linked to its structure, we found the

* To whom correspondence should be addressed. Phone: 301-217-4079. Fax: 301-217-5736. E-mail: craigt@nhgri.nih.gov. Address: Dr. Craig J. Thomas, NIH Chemical Genomics Center, NHGRI, National Institutes of Health 9800 Medical Center Drive, Building B, Room 3005, Mail Stop Code: 3370, Bethesda, MD 20892-3370.

[†] NIH Chemical Genomics Center, National Human Genome Research Institute, National Institutes of Health.

[‡] Molecular Immunology and Inflammation Branch, National Institute of Arthritis and Musculoskelatal and Skin Diseases, National Institutes of Health.

[§] Laboratory of Biological Modeling, National Institute of Diabetes and Digestive and Kidney Diseases, National Institutes of Health.

[∥] Transplantation and Autoimmunity Branch, National Institute of Diabetes and Digestive and Kidney Diseases, National Institutes of Health.

[⊥] Kelly Services.

[a] Abbreviations: Jak, Janus kinase; Tyk, Tyrosine kinase; IL, interleukin; Stat, signal transducers and activators of transcription; MCMM, Monte Carlo multiple minimum.

10.1021/jm801142b This article not subject to U.S. Copyright. Published 2008 by the American Chemical Society
Published on Web 11/19/2008

Scheme 1[a]

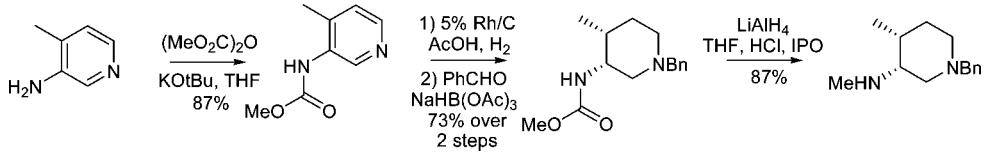

[a] Note: strategy and yields reflect those achieved and reported in *Org. Process Res. Dev.* **2005**, *9*, 51−56.

Scheme 2

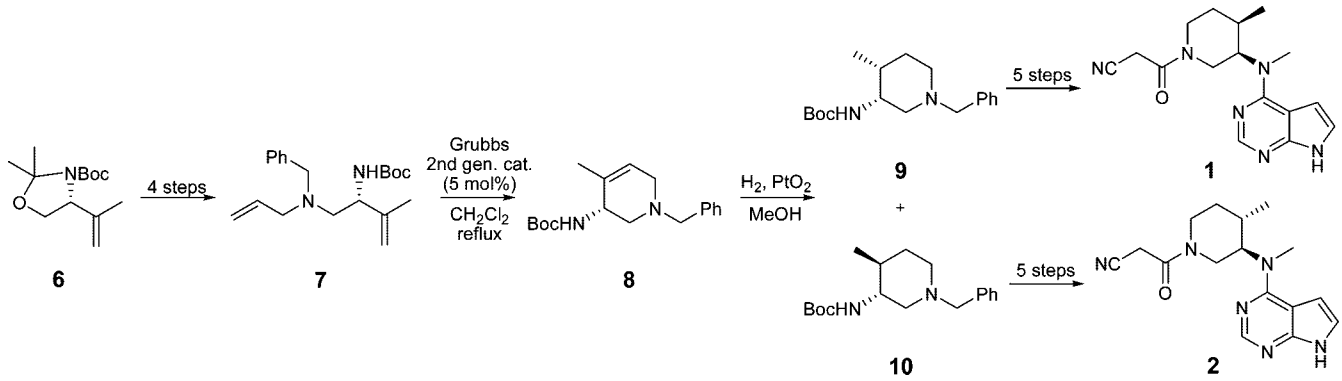

stereospecific nature of **1** and its selectivity against over 300 kinases to be of interest. Hoping to explore this facet of the molecule, we first set out to synthesize **1** and its three related stereoisomeric derivatives (analogues **2**, **3**, and **4**) (Figure 1).

Results

Synthesis of 1, 2, 3, and 4. The synthetic route undertaken by Pfizer has evolved to ultimately rely upon a 4-step transformation yielding the requisite (3*R*,4*R*)-1-benzyl-*N*,4-dimethylpiperidin-3-amine from 4-methylpyridin-3-amine (Scheme 1).[5] Crystallization with a di-*p*-toluoyltartrate salt was utilized to achieve enantiopurity following reduction of the substituted pyridine derivative. This route provides an elegant and efficient means to yield kilograms of the enantiomerically pure material needed for efficient production of **1**. It does not, however, provide a means to investigate 3,4-*trans* analogues of the piperidine ring. To explore the desired alternate stereochemical possibilities, we expanded upon a method described by Ledoussal and co-workers that relies upon the stereocenter that is set within Garner's aldehyde and a key step involving the ring-closing metathesis reaction (Scheme 2).[11] Here, the ultimate stereocenter at C3 of the piperidine ring is set by the choice of L-serine and utilizes precedented chemistry[12] to arrive at (*R*)-*tert*-butyl 2,2-dimethyl-4-(prop-1-en-2-yl)oxazolidine-3-carboxylate (**6**) (see Supporting Information for full synthetic details). Although several deviations from the reported work by Ledoussal and co-workers[11] were necessary, the general strategy provided (*R*)-*tert*-butyl 1-(allyl(benzyl)amino)-3-methylbut-3-en-2-ylcarbamate (**7**) in good yields. Application of the Grubbs second generation catalyst in refluxing dichloromethane afforded the requisite piperidine derivative **8** in yields typically exceeding 90%. Hydrogenation of the 3,4-alkene moiety resulted in the chromatographically separable piperidines **9** and **10**. Following separation, the remainder of the synthesis followed the synthetic strategy validated by White and co-workers to arrive at both **1** and **2**.[5] Utilizing D-serine as the starting material and following the same route allowed synthetic elaboration of **3** and **4**. Diastereomeric purity was examined via reverse phase HPLC analysis and enantiomeric purity was verified via chiral HPLC methods (see Supporting Information for details).

Inhibition of Stat5 Phosphorylation by 1, 2, 3, and 4. With **1** and its three related stereoisomeric derivatives (**2**, **3**, and **4**) in hand, we set out to ascertain each compounds ability to effectively inhibit Jak3. The Jak-Stat signaling pathway is a major regulatory element for gene transcription and plays a key role in processes such as immunoregulation and cellular proliferation and differentiation.[13] Jak3 natively associates with the common gamma chain γc forming a shared receptor for selected cytokines [including interleukin (IL)-2, IL-4, IL-7, IL-9, IL-15, and IL-21].[14] Upon cytokine binding, Jak3 is phosphorylated (presumably autophosphorylation), allowing signal transducers and activators of transcription (Stats) to bind to the cognate cytokine receptors via conserved Src homology 2 (SH2) domains.[15] Receptor-bound Stats are phosphorylated, dimerize (both homo and heterodimerization), and translocate to the nucleus to trigger gene transcription. To examine cellular Jak3 activity directly, we analyzed enriched, human CD4+ T cells isolated from PBMC's incubated with each compound at relevant concentrations (5, 50, and 500 nM) and a DMSO control prior to stimulation with IL-2. The degree of Stat5 phosphorylation was analyzed from cell lysates via immunoblotting with an antiphospho-Stat5 mAb (antiactin mAb was performed as a control to confirm equal protein loading) (Figure 2, left blot). From this experiment, it was clear that only **1** maintained the ability to affect Stat5 phosphorylation at the concentrations tested, highly suggesting that the alternate stereochemical configurations of the molecule had deleterious effects on Jak3 inhibition.

IL-12 is another important immunoregulatory cytokine. The IL-12 receptor comprises two subunits that associate with Jak2 and Tyk2 and activates Stat4.[16,17] A primary selectivity issue for **1** is its reported downregulation of Jak2. We examined the ability of each compound to block the phosphorylation of Stat4 within IL-12 stimulated cells (Figure 2, right blot). The results demonstrate no clear inhibition by **1** or its related stereoisomers. This suggests that **1** is capable of selectively inhibiting Jak3 without disrupting the functions of Jak2 or Tyk2 in a cellular environment at the concentrations tested.

Analysis of Kinase Selectivity. To fully understand these compounds potential, we pursued a direct analysis of each

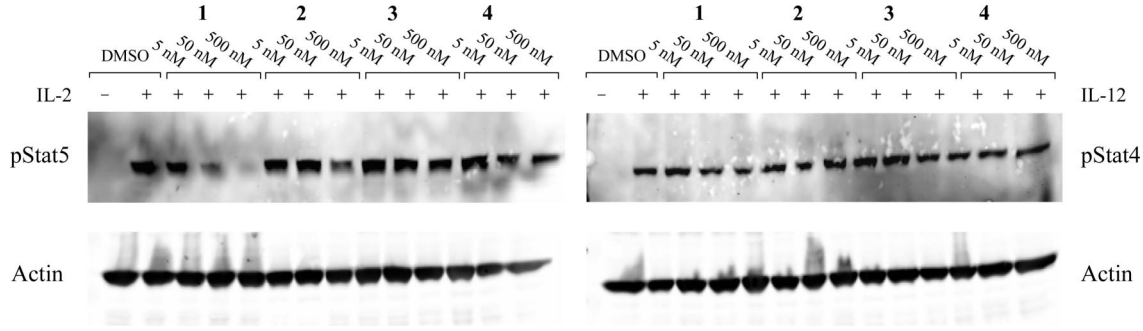

Figure 2. Gel analysis showing the inhibitory ability of **1**, **2**, **3**, and **4** to disrupt Stat5 phosphorylation (left blot) or Stat4 phosphorylation (right blot) in human CD4+ cells. CD4+ T cells were rested and incubated with DMSO control (lane 2), **1** (lane 3−5), **2** (lane 6−8), **3** (lane 9−11), or **4** (lane 12−14) at increasing concentrations (5, 50, and 500 nM, respectively) for 1 h before being stimulated with IL-2 (1000 μg/mL; left blot) or IL-12 (100 ng/mL; right blot) for 15 min or incubated in medium without cytokine stimulation (lane 1; both gels). Cell lysates were partitioned, stripped, and immunoblotted with antiphospho-Stat5 (rabbit) mAb (left blot, top gel) or antiphospho-Stat4 (rabbit) mAb (right blot, top gel). Antiactin mAb (mouse) was used to confirm equal loading of protein across lanes (bottom gels).

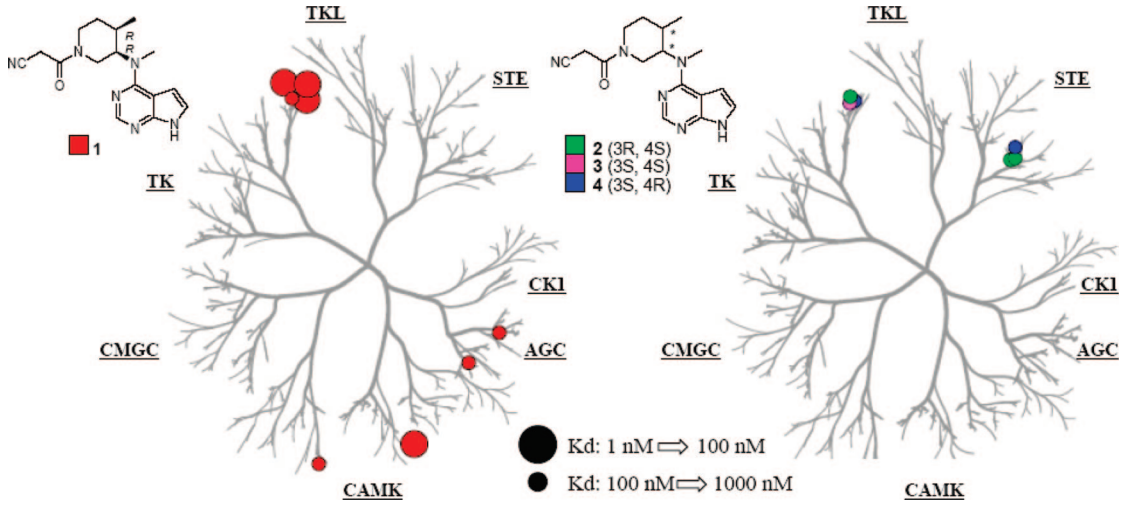

Figure 3. Dendrogram representation of the selectivity profile for kinase inhibition by **1** and stereoisomers **2**, **3**, and **4** within a panel of 354 kinases. Activity for **1**: DCamKL3 = 4.5 nM, Jak1 = 3 nM, Jak2 = 2 nM, Jak3 = 0.7 nM, Tyc2 = 250 nM, Pkn1 = 200 nM, Snark = 420 nM, Tnk1 = 640 nM. Activity for **2**: Jak2 = 600 nM, Jak3 = 190 nM, Mst1 = 250 nM, Mst2 = 450 nM. Activity for **3**: Jak2 = 270 nM, Jak3 = 180 nM. Activity for **4**: Jak2 = 420 nM, Jak3 = 150 nM, Map4K3 = 460 nM, Map4K5 = 790 nM.

stereoisomer against purified Jak3. Further, **1** represents a novel and unique chemotype for kinase inhibition and it was of interest to profile each stereoisomer across a panel of kinases. Recently, Ambit Biosciences reported the aforementioned quantitative analysis of 38 known kinase inhibitors (including **1**) across a panel of 317 kinases.[9] We submitted **1** and the stereoisomeric analogues **2**, **3**, and **4** across the same panel (at present containing 354 kinases). The initial profile provides activity as a percentage of DMSO control (for the full report, see the Supporting Information). Activities beyond a selected threshold were submitted for K_d determinations, and the results are shown as a dendrogram representation in Figure 3. The profile of **1** closely matched the published data [with 2 notable exceptions: Mst2, "no hit" (reported IC50 of 4.2 μM), and Tyk2, "no hit" (reported IC50 of 620 nM)]. The profile additionally found a K_d of 210 nM for **1** at Rock (Rock was not part of the original 317 kinases screened in ref 9). Full K_d determinations for **1** were pursued for the four related Jak targets as well as the Jak1 (JH2domain-pseudokinase). These results confirmed that **1** binds Jak3 and Jak2 nearly equipotently (K_d of 0.75 nM for Jak3 and a K_d of 1.8 nM for Jak2). The disassociation constants for **1** at Jak1 and Tyk2 were recorded at 1.7 and 260 nM, respectively (as compared to the earlier report of 640 nM binding at Tyk2). No affinity was observed for **1** at the Jak1 (JH2domain-pseudokinase). These data contrast sharply with the original report denoting a higher degree of selectivity for Jak3 over Jak2 and Jak1. Interestingly, these results conflict with the cell-based study showing little or no inhibition of Stat4 phosphorylation by **1**.

The profile results for **2**, **3**, and **4** indicate that each stereoisomer retains a degree of affinity for Jak3 and Jak2, although the potency of the interaction drops significantly. The profile for **3** (the enantiomer of **1**) showed solitary activity at Jak3 and Jak2 (K_d's of 180 and 270 nM, respectively). Enantiomers **2** and **4** had similar K_d's for Jak3 and Jak2 but also maintained several novel interactions. For instance, **2** was found to have modest binding potential for Mst1 and Mst2 (K_d's of 320 and 450 nM, respectively). Analogue **4** was found to have modest binding at Map4K3 and Map4K5 (K_d's of 460 and 790 nM, respectively). Mst and Map4K kinase subfamilies reside on the related STE20 and STE7 branches of the kinome. That enantiomers **2** and **4** show activity at these related targets, suggesting that this chemotype may represent a novel starting point for the development of selective inhibitors of these important kinase classes.

Minimum Energy Conformations of Unbound 1, 2, 3, and 4 in Water. Chirality, pharmacology, and drug discovery are intertwining subjects dating back to the early use of quinine, atropine, and opiates to several of today's best known drugs. In each instance, the chiral nature of these small molecules plays

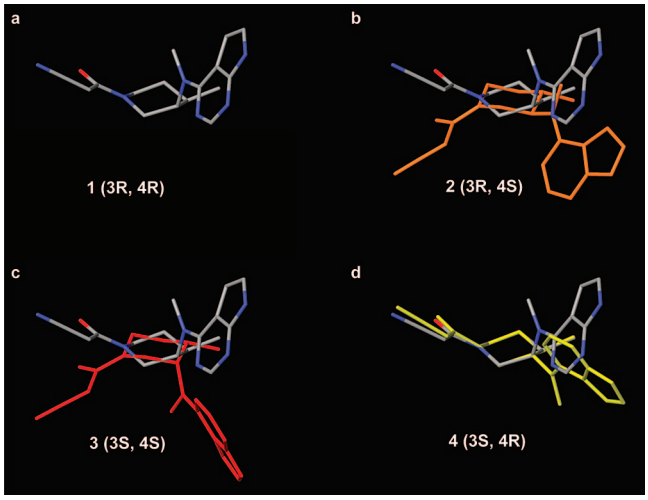

Figure 4. Molecular models of the lowest energy conformers of **1**−**4** generated through Monte Carlo conformational searches. The model of **1** is colored by atom type (gray: carbon; red: oxygen; blue; nitrogen), while the models of **2**, **3**, and **4** are colored orange, red, and yellow, respectively. Compounds **2**, **3**, and **4** are overlapped to **1** by superimposition of the six member ring atoms. All compounds prefer the chair conformation; however, **1** and **4** show a θ of ∼180°, while **3** and **2** adopt the diametrically opposite chair conformation, with a θ of ∼0°.

a role in their biochemical efficacy. With a deeper understanding of the chiral nature of **1** and its kinase selectivity profile, we explored the role of the (4*R*)-methyl substituent and the (3*R*)-deazapurine moiety in defining its minimum energy conformation and how this probable conformation facilitates binding to Jak3.

The conformational space of the unbound inhibitors **1**−**4** was studied by subjecting the molecules to two consecutive Monte Carlo multiple minimum (MCMM) conformational searches (initially in vacuo, subsequently in implicit water). The resulting minimum energy models are shown in Figure 4 and can be discussed utilizing the truncated Fourier (TF) series-based coordinates for the description of six-membered ring puckering established by Haasnoot[18] (plots representing the azimuthal θ angles, the two torsional angles describing the orientation of the base, and percentage energy increase of the various conformers obtained for **1**−**4** and are provided in the Supporting Information). The six-membered ring of all the compounds can adopt two diametrically opposite chair conformations, represented by θ angles of 0° and 180°. Enantiomers **1** and **3**, which have the methyl substituent and the base on the same side of the ring plane, show a clear preference for having the methyl substituent in an equatorial position and the deazapurine moiety in an axial position (preferred θ of ∼180° for **1** and ∼0° for **3**). Enantiomers **2** and **4** position these substituents on opposing sides of the plane of the piperidine ring conferring a stronger preference for having the two substituents in equatorial positions (preferred θ of ∼0° and ∼180° for **2** and **4**, respectively). Interestingly, the signal for piperidine ring C3−H of **1** was noted at 4.78 ppm, while the C3−H of **2** was found at 4.32 ppm (assigned via COSY analysis). The relative downfield shift in **1** highly suggests a more equatorial character for the C3−H of **1** and relative axial character for the C3−H of **2**, which is consistent with the results from the MCMM searches.

Using the deazapurine base as the anchor point for discussion (and likely for binding to Jak3), it is clear that even the fairly "minor" change of the stereochemical configuration of the methyl group in structures **1** and **2** results in significant changes in the ultimate three-dimensional structures of these agents. This broadly accepted phenomenon is intensified when placing chiral substituents on five- and six-membered ring structures due to hypersensitivity in ring conformations.

Docking of 1, 2, 3, and 4 at Jak3. There are four members of the Jak family of kinases; Jak1, Jak2, Jak3, and Tyrosine kinase 2 (Tyk2).[15] Each member of this family retains seven conserved sequence regions (or Jak homology domains): the JH1 domain (or kinase domain), the JH2 domain (or pseudokinase domain), the JH3 and JH4 domains (both are SH2 domains), and JH6 and JH7 domains (collectively, the FERM domain or four-point-one, ezrin, radixin, and moesin homology domain).[13,15] In 2005, Boggon et al. reported the crystal structure for the Jak3 kinase domain bound to a staurosporine analogue **23** (AFN941).[19]

Utilizing this structure as a template, the four stereoisomers **1**−**4** were docked at the Jak3 catalytic cleft using Glide 4.5 in order to shed light on the mechanistic preference for the binding of **1**.[20] In particular, on the basis of the crystallographic coordinates of the Jak3−**23** complex, the inhibitors were docked at the ATP-binding site, lined by residues from the N-terminal lobe on the roof of the pocket (Leu828, Gly829, Val836, and Ala853), the C-terminal lobe on the floor of the pocket (Leu956, Gly908, and Cys909), and the hinge region (from Met902 to Leu905). The opening of the cleft is defined by hydrophilic residues like Arg953, Asn954, Asp949, and Gln988. Interactions with residue backbones of the hinge region define the binding motif of many kinase inhibitors (including **23** with Jak3). We, therefore, utilized specified hydrogen bonds between Glu903 and Leu905 and each stereoisomer as a criterion for retrieving the ligand poses from the docking results along with the docking score and the energetic contributes to the binding interactions.

The results from the highest scoring Jak3−**1** docking complex are shown in Figure 5 and illustrate that the N3 and N9 nitrogens of the 7-deazapurine moiety participate in key hydrogen bonds with residues Glu903 and Leu905. These interactions mimic hydrogen bonds found within the crystal structure of Jak3 with **23**. Another significant interaction involves hydrogen bonds formed between the nitrile function and Arg953 at the opening of the cleft. This docking pose further validates the notion that the 4*R*-methyl group occupies an equatorial position while the 3*R*-base moiety is directed into an axial position in the chair conformation of the piperidine ring.

Comparing the docking poses for **1**, **2**, **3**, and **4** found in the highest scoring Jak3 docking complexes to the minimum energy structures of the unbound **1**, **2**, **3**, and **4** from the conformational analyses provides valuable insight into the superior binding associated with the (3*R*,4*R*) stereochemical configuration of **1**. Figure 6 shows the predicted unbound conformation for each compound overlaid with the conformation associated with docking at Jak3. From this rendering, it is clear that only **1** docks with Jak3 in a conformation that extensively resembles the compounds minimum energy conformation (Figure 6a). For **2**, the six-membered ring assumes a half-chair conformation with both the substituent in equatorial position (Figure 6b). Compound **3** docked with the six-membered ring in a chair conformation and, contrary to the conformational preferences revealed by the MCMM search, the methyl and base substituents were found in the axial and equatorial position, respectively (Figure 6c). Finally, compound **4** docked with the six-membered ring in a twist-boat conformation with both methyl and base substituents in the equatorial position (Figure 6d). These data indicate that compounds **2**, **3**, and **4** are forced to adopt unlikely

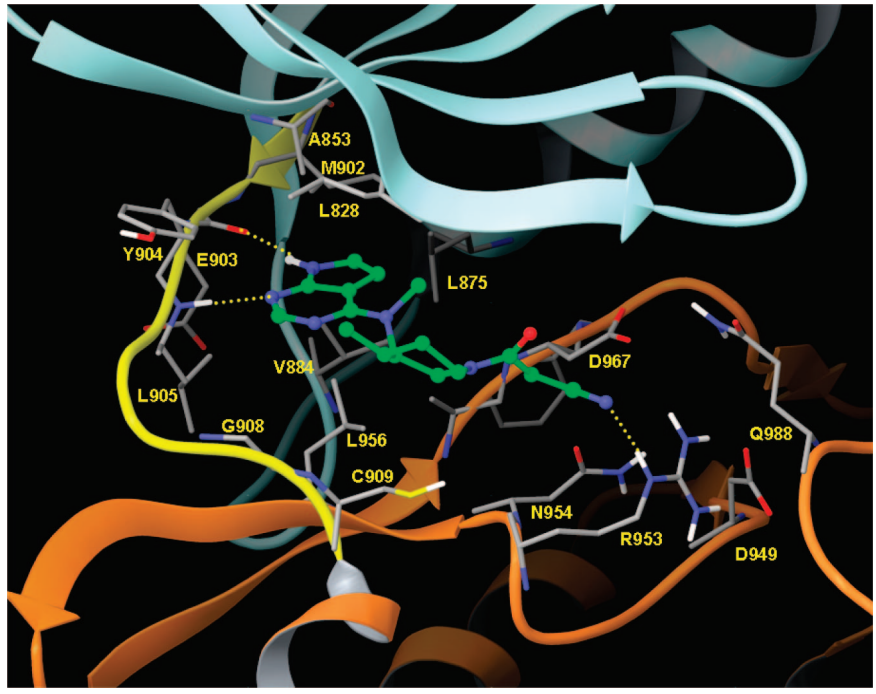

Figure 5. Proposed binding mode of **1** in the catalytic site of Jak3. The protein is shown with the ribbons representation with the N-lobe colored in cyan, the C-lobe in orange, and the hinge region in yellow. The residues in the binding pocket are colored by atom type. Compound **1** is shown as ball-and-stick model with carbon atoms colored in green. The major polar interactions between compound **1** and the residues in the pocket are highlighted as dotted lines.

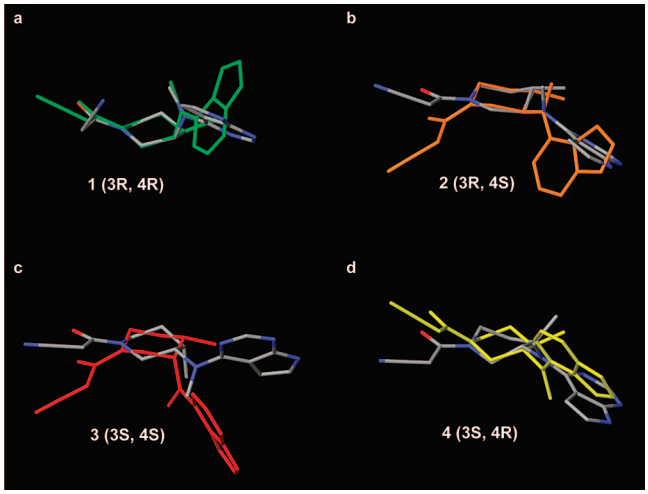

Figure 6. Superposition of the six-membered ring between the lowest energy conformation of compounds **1**−**4** (colored in green, orange, red, and yellow) and the respective best scored docking poses (colored by atom type).

high energy conformations in order to bind effectively at the Jak3 catalytic site.

Discussion

Inhibition of Jak3 and Jak2 by 1. Jak3 represents an intriguing therapeutic target.[21] Jak3 is primarily expressed within T cells and NK cells and specific mutations to Jak3 result in $T^-B^+NK^-$ severe combined immunodeficiency (SCID).[22] Unsurprisingly, the knockout phenotype for Jak3 is a viable but immunocompromised animal.[23] Conversely, Jak2 is ubiquitously expressed and knockouts are embryonic lethal.[24] Given these data, substantial effort has been invested in the search for highly selective Jak3 inhibitors.

Jak2 possesses a high degree of homology to Jak3 (47%) and is particularly homologous at the kinase active site.[19] Comparison between the catalytic pockets of crystal structures of Jak3 and Jak2 revealed conformational differences in the glycine-rich loop and the activation loop that result in a rather tighter pocket for Jak2. Docking of **1** within the crystal structure of the catalytic cleft of Jak2[25] (see Supporting Information) suggests that the complexes of **1** with both Jak3 and Jak2 are decidedly similar. Only three residues in spatial proximity to the binding site of **1** at Jak3 and Jak2 are divergent: Jak3 Ala966−Jak2 Gly993, in proximity of the DFG motif, Jak3 Cys909−Jak2 Ser936, at the end of the hinge region, and Jak3 Gln988−Jak2 Glu1015, in the activation loop. Cycles of MCMM conformational search performed on the Jak3−**1** complex, granting flexibility to the ligand and the residues within a 4 Å radius allow for a potential hydrogen bond between the nitrile function and Gln988, an interaction that would be missing in Jak2. However, the docking pose of **1** in Jak2 does retain the key hydrogen bond with Arg980 (Arg953 in Jak3).

It is unclear how this lone deviation may affect binding, but given the relative K_d and IC_{50} values reported for **1** at both targets, the difference is presumably negligible. This is also consistent with the fact that, due to the different conformation of the portion of the activation loop located immediately prior to the APE motif, in Jak2 Glu1015 points away from the binding site and would not be in proximity with the nitrile moiety.

From the docking comparisons, the similar disassociation constants for **1** at Jak3 and Jak2 are not surprising. Early results from the clinical use of **1** demonstrate efficacy but also unwanted anemia and neutropenia.[26] This suggests that unwelcome downregulation of Jak2 is occurring to an appreciable extent. Nonetheless, phase 1 clinical evaluations demonstrated a reasonable safety profile and numerous phase 2 evaluations are currently underway. The IC_{50} values reported by Changelian et al. indicate a small degree of selectivity between Jak3 and Jak2 (1 nM for Jak3 versus 20 nM for Jak2). It is unclear if the selectivity differences noted in these studies are the result of the relative Km (ATP) of each kinase. Nonetheless, whether **1**

binds/inhibits Jak2 at 1 or 20 nM concentrations, it is likely that the physiological levels of the drug will surpass the amount needed for effective downregulation of Jak2. The more compelling experiments, however, are cell-based studies such as the assessment of inhibition of Stat4 phosphorylation by **1** (Figure 2) and the previous report that **1** effectively inhibits IL-2 stimulated cell proliferation (Jak3 dependent) while having much weaker effect on granulocyte macrophage-colony stimulation factor induced proliferation (Jak2 dependent). It remains to be seen if these results provide clues into the method by which cytokine receptor/Jak pairs initiate signaling cascades.

Conclusion

Kinases are among the most intriguing therapeutic targets in the human proteome and kinase inhibitors are becoming staples of the pharmacopeia. A primary doctrine of drug design is to limit the number of chiral centers placed into small molecules intended for clinical use for a myriad of reasons. **1** goes against convention and incorporates not one, but two chiral centers. Using a combination of molecular modeling, target profiling and cell-based analyses we have shown that the chiral nature of **1** is a key facet that defines its ability to bind and inhibit its primary target. Additionally, discrete stereoisomers of **1** may prove useful starting points for novel small molecules targeting alternate branches of the kinome. Finally, the divergence of activity for **1** in purified protein assays versus cell-based assays remains an intriguing characteristic of this compound and should be explored further.

Methods

Synthesis of 1, 2, 3, and 4. Complete procedures for the synthesis of **1**, **2**, **3**, and **4** are presented in the Supporting Information. The general strategy followed precedented chemistry from refs, 5, 11, and 12. Analysis of diastereopurity and enantiopurity were determined through reverse phase and chiral phase HPLC methods. Proton NMR for all enantiomers was identical.

3-((3*R*,4*R*)-3-((1*H*-Indol-4-yl)(methyl)amino)-4-methylpiperidin-1-yl)-3-oxopropan-enitrile (1). $[\alpha]_D^{25} = +10.4$ (*c* 0.64, MeOH); NMR spectra are complicated due to amide rotomers. ^{1}H NMR (400 MHz, $CDCl_3$) δ 12.67 and 12.63 (s, 1H), 8.39 and 8.37 (s, 1H), 7.40−7.44 (m, 1H), 6.80−6.90 (m, 1H), 4.78 (brs, 1H), 4.08−4.20 and 3.96−4.06 (m, 2H), 3.68−3.86 (m, 2H), 3.37−3.46 and 3.14−3.22 (m, 2H), 3.35 (s, 3H), 2.34−2.46 (m, 1H), 1.76−1.95 (m, 1H), 1.52−1.67 (m, 1H), 1.07 and 1.04 (d, $J = 7.4$ Hz, 3H). ^{13}C NMR (100 MHz, $CDCl_3$) δ 162.52 and 162.46, 159.3, 159.0, 145.4 and 145.1, 124.0 (br), 117.0 and 116.9, 105.2 and 104.9, 102.7, 56.8 and 55.7, 45.2, 43.1 and 42.1, 38.7 and 35.8, 31.8 and 31.4, 30.7, 25.8 and 25.7, 14.4 and 13.9. IR (neat) 3130, 2965, 1619, 1535, 1452, 1197, 1134, 1053, 906, 838, 720 cm^{-1}. HRMS (FAB) Calcd for $C_{16}H_{21}N_6O$ (M + H) 313.1777, found 313.1778.

3-((3*R*,4*S*)-3-((1*H*-Indol-4-yl)(methyl)amino)-4-methylpiperidin-1-yl)-3-oxopropane- nitrile (2). $[\alpha]_D^{25} = +74.8$ (*c* 0.60, MeOH); the NMR are complicated due to the rotamers of the amide. ^{1}H NMR (400 MHz, $CDCl_3$) δ 12.58 (brs, 1H), 8.38 and 8.37 (s, 1H), 7.42 (s, 1H), 6.96 and 6.87 (d, $J = 2.4$ Hz, 1H), 4.32 (brs, 1H), 3.96−4.16 (m, 2H), 3.62−3.72 (m, 1H), 3.37 and 3.31 (s, 3H), 3.05−3.16 (m, 1H), 2.86−2.98 (m, 1H), 2.62−2.76 (m, 1H), 2.06−2.22 (m, 1H), 1.78−1.87 (m, 1H), 1.18−1.32 and 1.34−1.48 (m, 1H), 0.85 and 0.80 (d, $J = 6.4$ Hz, 3H). ^{13}C NMR (100 MHz, $CDCl_3$) δ 162.6 and 162.4, 159.3, 159.0, 145.7 (br), 124.0 (br), 117.0 and 116.9, 105.1 and 104.7, 102.5, 47.3 and 46.1, 43.7, 42.5, 41.3, 33.6, 33.0 and 32.9, 25.9 and 25.8, 18.5. IR (neat) 3123, 2963, 1599, 1541, 1452, 1198, 1137, 1056, 907, 830, 720 cm^{-1}. HRMS (FAB) Calcd for $C_{16}H_{21}N_6O$ (M + H) 313.1777, found 313.1775.

Profiles of 1, 2, 3, and 4. Kinase profiles were performed by Ambit Biosciences (San Diego, CA: http://www.ambitbio.com/) utilizing KINOME*scan*. Activity is recorded via a competition binding assay of selected kinases that are fused to a proprietary tag. Measurements of the amount of kinase bound to an immobilized, active-site directed ligand in the presence and absence of the test compound provide a % of DMSO control for binding of ligand. Activities between 0 and 10 were selected for K_d determinations. Dendrogram representations were generated by an in-house visualization tool designated PhyloChem. Dendrogram clustering and apexes are based on the human phylogenetic kinase data available at http://kinase.com/human/kinome.

Analysis of Stat5 and Stat4 Phosphorylation. Human CD4+ positive cells were enriched from peripheral blood mononuclear cells obtained from a healthy donor by magnetic separation (CD4+ MACS beads). CD4+ cells were activated for 3 days with plate bound anti-CD3 and anti CD28 antibodies (5 ug/mL each) and then expanded for another 4 days in the presence of IL-2 (50 U/mL). Cells were rested overnight in 1% RPMI and preincubated with **1**, **2**, **3**, **4** or DMSO control for 1 h at indicated concentrations [(5, 50, 500 nM) DMSO concentration was equal in all preparations] and then activated with IL-2 (1000 μg/mL) or IL-12 (100 ng/mL) for 15 min. Cells (10×10^6/condition) were lysed in 1% Triton-X lysis buffer and equal amounts of cell lysate were run in NuPage Bis-Tris gel (4−12% gradient). Proteins were transferred onto nitrocellulose membrane. Detection was done with indicated antibodies using Odyssey Western blotting system according to manufacturer's instructions. [http://www.licor.com/bio/QuantitativeWesterns/index.jsp] Primary antibodies used: antiactin mouse mAb (Chemicon), 1:5000, antiphospho-Stat5 rabbit mAb (Cell Signaling), antiphospho-Stat4 (Zymed) 1:1000, and secondary goat-antimouse IgG Ab (Rockland) and goat-antirabbit IgG (Molecular Probes).

Monte Carlo Conformational Searches. Compounds **1**−**4** were sketched in Maestro and subjected to 100 steps of Monte Carlo multiple minimum (MCMM) conformational search performed in vacuo by means of MacroModel (Schrödinger LLC, New York, NY, 2007).[27,28] The lowest energy conformer was subsequently used as the starting point for additional 1000 steps of MCMM search, this time performed using water as implicit solvent (surface generalized Born model). All calculations were conducted with the OPLS_2005 force field.

Protein Preparation. The X-ray crystallographic structure of the human Jak3 kinase domain in a catalytically active state and in complex with the staurosporine derivative **23** was retrieved from the Protein Data Bank (PDB code: 1YVJ, atomic resolution 2.55 Å).[19] The protein structure was prepared for the docking studies using the Protein Preparation Wizard tool implemented in Maestro (Schrödinger LLC, New York, NY, 2007). All crystallographic water molecules and other chemical components were deleted, the right bond orders were assigned, and the hydrogen atoms were added to the protein. Arginine and lysine side chains were considered as cationic at the guanidine and ammonium groups, and the aspartic and glutamic residues were considered as anionic at the carboxylate groups. The hydrogen atoms were subsequently minimized employing the Polak−Ribiere conjugate gradient (PRCG) method until a convergence to the gradient threshold of 0.05 kJ/(mol Å). The atomic charges were computed using the OPLS_2005 force field.

Molecular Docking. All compounds were docked inside the active site of Jak3 using Glide 4.5,[20] the automated docking program implemented in the Schrödinger package (Schrödinger LLC, New York, NY, 2007). The binding site was defined around the position occupied by the cocrystallized ligand in the Jak3 complex structure 1YVJ. In the receptor grid generation, a $10 \times 10 \times 10$ Å^3 cubic docking box was generated and the known H-bond interactions between most of the kinase inhibitors and the backbone of the hinge segment were enforced, defining the backbone amino groups of Leu905 and the backbone carboxylic groups of Glu903 as potential H-bond donor and acceptor respectively. The XP mode of Glide was utilized. The obtained complexes between Jak3 and the best scored pose of each compound were then submitted to 1000 steps of MCMM conformational search performed with the OPLS_2005

force field. The energy minimization was employed with PRCG procedure until convergence to the gradient threshold of 0.05 kJ/(mol Å). The reproduction of the binding mode of **23** in the catalytic site of Jak3 as in the crystallographic structure 1YVJ (rmsd value about 0.43 Å) validated the docking and MCMM search protocol used for this study.

Acknowledgment. We thank Dr. David Maloney and Dr. Douglas Auld for advice and help during the preparation of this manuscript. We thank Allison Peck for critical reading of this manuscript. This research was supported by the Molecular Libraries Initiative of the National Institutes of Health Roadmap for Medical Research, the Intramural Research Program of the National Human Genome Research Institute, the National Institute of Arthritis and Musculoskeletal and Skin Diseases, and the National Institute of Diabetes and Digestive and Kidney Diseases, National Institutes of Health.

Supporting Information Available: Synthetic procedures, selected spectra, expanded experiments and complete profile results. This material is available free of charge via the Internet at http://pubs.acs.org.

References

(1) Changelian, P. S.; Flanagan, M. E.; Ball, D. J.; Kent, C. R.; Magnuson, K. S.; Martin, W. H.; Rizzuti, B. J.; Sawyer, P. S.; Perry, B. D.; Brissette, W. H.; McCurdy, S. P.; Kudlacz, E. M.; Conklyn, M. J.; Elliot, E. A.; Koslov, E. R.; Fisher, M. B.; Strelevitz, T. J.; Yoon, K.; Whipple, D. A.; Sun, J.; Munchhof, M. J.; Doty, J. L.; Casavant, J. M.; Blumenkopf, T. A.; Hines, M.; Brown, M. F.; Lillie, B. M.; Subramanyam, C.; Shang-Poa, C.; Milici, A. J.; Beckius, G. E.; Moyer, J. D.; Su, C.; Woodworth, T. G.; Gaweco, A. S.; Beals, C. R.; Littman, B. H.; Fisher, D. A.; Smith, J. F.; Zagouras, P.; Magna, H. A.; Saltarelli, M. J.; Johnson, K. S.; Nelms, L. F.; Des Etages, S. G.; Hayes, L. S.; Kawabata, T. T.; Finco-Kent, D.; Baker, D. L.; Larson, M.; Si, M.-S.; Paniagua, R.; Higgins, J.; Holm, B.; Reitz, B.; Zhoa, Y.-J.; Morris, R. E.; O'Shea, J. J.; Borie, D. C. Prevention of Organ Allograft Rejection by a Specific Janus Kinase 3 Inhibitor. *Science* **2003**, *302*, 875–878.

(2) Blumenkopf, T. A.; Flanagan, M. E.; Munchhof, M. J. Patent EP 1235830, 2004; Japanese Patent JP 2003516405, 2003; U.S. Patent US 2001053782 2001; U.S. Patent US6627754, 2003; Patent WO 0142246, 2001.

(3) Ruggeri, S. G.; Hawkins, J. M.; Makowski, T. M.; Rutherford, J. L.; Urban, F. J. Japanese Patent JP 2007039455, 2007; Patent WO 2007012953, 2007.

(4) Flanagan, M. E.; Li, Z. J. Japanese Patent JP 2005511696, 2005; U.S. Patent US 2003130292, 2003; Patent WO 03048162, 2003.

(5) Cai, W.; Colony, J. L.; Frost, H.; Hudspeth, J. P.; Kendall, P. M.; Krishnan, A. M.; Makowski, T.; Mazur, D. J.; Phillips, J.; Ripin, D. H. B.; Ruggeri, S. G.; Stearns, J. F.; White, T. D. Investigation of Practical Routes for the Kilogram-Scale Production of *cis*-3-Methylamino-4-methylpiperidines. *Org. Process Res. Dev.* **2005**, *9*, 51–56.

(6) Sorbera, L. A.; Serradell, N.; Bolós, J.; Rosa, E.; Bozzo, J. CP-690,550. *Drugs Future* **2005**, *32*, 674–680.

(7) Busque, S.; Leventhal, J.; Brennan, D.; Klintmalm, G.; Steinberg, S.; Shah, T.; Lawendy, N.; Wang, C.; Chan, G. CP-690,550 (CP), a Jak3 Inhibitor, in de Novo Kidney Transplant (KT) Recipients: 6-Month Results of a Phase 2 Trial. *Am. J. Transplant* **2007**, (s2), 304.

(8) Kremer, J. M.; Bloom, B. J.; Breedveld, F. C.; Coombs, J.; Fletcher, M. P.; Gruben, D.; Krishnaswami, S.; Burgos-Vargas, R.; Wilkinson, B.; Zerbini, C. A. F.; Zwillich, S. H. A randomized, double-blind, placebo-controlled trial of 3 dose levels of CP-690,550 versus placebo in the treatment of acute rheumatoid arthritis, *70th Annu. Sci. Meeting Am. Coll. Rheumatol.* 2007, Abstract L40.

(9) Karaman, M. W.; Herrgard, S.; Treiber, D. K.; Gallant, P.; Atteridge, C. E.; Campbell, B. T.; Chan, K. W.; Ciceri, P.; Davis, M. I.; Edeen, P. T.; Faraoni, R.; Floyd, M.; Hunt, J. P.; Lockhart, D. J.; Milanov, Z. V.; Morrison, M. J.; Pallares, G.; Patel, H. K.; Pritchard, S.; Wodicka, L. M.; Zarrinkar, P. P. A quantitative analysis of kinase inhibitor selectivity. *Nat. Biotechnol.* **2008**, *26*, 127–132.

(10) Changelian, P. S.; Moshinsky, D.; Kuhn, C. F.; Flanagan, M. E.; Munchhof, M. J.; Harris, T. M.; Doty, J. L.; Sun, J.; Kent, C. R.; Magnuson, K. S.; Perregaux, D. G.; Sawyer, P. S.; Kudlacz, E. M. The specificity of Jak3 kinase inhibitors. *Blood* **2008**, *111*, 2155–2157.

(11) Hu, X. E.; Kim, N. K.; Ledoussal, B. Synthesis of *trans*-(3*S*)-Amino-(4*R*)-alkyl−and−(4*S*)-Aryl-piperidines via Ring-Closing Metathesis Reaction. *Org. Lett.* **2002**, *4*, 4499–4502.

(12) Williams, L.; Zhang, Z.; Shao, F.; Carroll, P. J.; Joullié, M. M. Grignard Reactions to Chiral Oxazolidine Aldehydes. *Tetrahedron* **1996**, *52*, 11673–11694.

(13) Yamaoka, K.; Saharinen, P.; Pesu, M.; Holt, V. E. T., III; Silvennoinen, O.; O'Shea, J. J. The Janus kinases (Jaks). *Genome Biol.* **2004**, *5*, 253.1253.6.

(14) O'Shea, J. J.; Park, H.; Pesu, M.; Borie, D.; Changelian, P. New strategies for immunosuppression: interfering with cytokines by targeting the Jak/Stat pathway. *Curr. Opin. Rheumatol.* **2005**, *17*, 305–311.

(15) Bhandari, R.; Kuriyan, J. Jak-Stat signaling. In *Handbook of Cell Signaling*, 1st ed.; Bradshaw, R., Dennis, E., Eds.; Academic Press: New York, 2003; 343−347.

(16) Bacon, C. M.; McVicar, D. W.; Ortaldo, J. R.; Rees, R. C.; O'Shea, J. J.; Johnston, J. A. Interleukin 12 (IL12) Induces Tyrosine Phosphorylation of JAK2 and TYK2: Differential Use of Janus Family Tyrosine Kinases by IL-2 and IL-12. *J. Exp. Med.* **1995**, *181*, 399–404.

(17) Bacon, C. M.; Petricoin, E. F., III; Ortaldo, J. R.; Rees, R. C.; Larner, A. C.; Johnston, J. A.; O'Shea, J. J. Interleukin 12 induces tyrosine phosphorylation and activation of STAT4 in human lymphocytes. *Proc. Natl. Acad. Sci. U.S.A.* **1995**, *92*, 7307–7311.

(18) Haasnoot, C. A. G. The Conformation of Six-Membered Rings Described by Puckering Coordinates Derived from Endocyclic Torsion Angles. *J. Am. Chem. Soc.* **1992**, *114*, 882–887.

(19) Boggon, T. J.; Li, Y.; Manley, P. W.; Eck, M. J. Crystal Structure of the Jak3 kinase domain in complex with a staurosporine analog. *Blood* **2005**, *106*, 996–1002.

(20) *Glide 4.5*; Schrödinger, LLC: New York, 2007.

(21) Podder, H.; Kahan, B. D. Janus kinase 3: a novel target for selective transplant immunosuppression. *Expert Opin. Ther. Targets* **2004**, *8*, 613–629.

(22) Russell, S. M.; Tayebi, N.; Nakajima, H.; Riedy, M. C.; Roberts, J. L.; Aman, M. J.; Migone, T.-S.; Noguchi, M.; Markert, L.; Buckley, R. H.; O'Shea, J. J.; Leonard, W. J. Mutations of Jak3 in a Patient with SCID: Essential Role of Jak3 in Lymphoid Development. *Science* **1995**, *270*, 797–800.

(23) Thomis, D. C.; Gurniak, C. B.; Tivol, E.; Sharpe, A. H.; Berg, L. J. Defects in B lymphocyte maturation and T lymphocyte activation in mice lacking Jak3. *Science* **1995**, *270*, 794–797.

(24) Neubauer, H.; Cumano, A.; Muller, M.; Wu, H.; Huffstadt, U.; Pfeffer, K. Jak2 deficiency defines an essential developmental check-point in definitive hematopoiesis. *Cell* **1998**, *93*, 397–409.

(25) Lucet, I. S.; Fantino, E.; Styles, M.; Bamert, R.; Patel, O.; Broughton, S. E.; Walter, M.; Burns, C. J.; Treutlein, H.; Qilks, A. F.; Rossjohn, J. The structural basis of Janus kinase 2 inhibition by a potent and specific pan-Janus kinase inhibitor. *Blood* **2006**, *107*, 176–183.

(26) Liu, E. H.; Siegel, R. M.; Harlan, D. M.; O'Shea, J. J. T cell-directed therapies: lessons learned and future prospects. *Nat. Immunol.* **2007**, *8*, 25–30.

(27) Chang, G.; Guida, W. C.; Still, W. C. An Internal Coordinate Monte Carlo Method for Searching Conformational Space. *J. Am. Chem. Soc.* **1998**, *111*, 4379–4386.

(28) Mohamadi, F.; Richards, N. G. J.; Guida, W. C.; Liskamp, R.; Lipton, M.; Caufield, C.; Chang, G.; Hendrickson, T.; Still, W. C. Macromodel−An Integrated Software System for Modelling Organic and Bioorganic Molecules Using Molecular Mechanics. *J. Comput. Chem.* **1990**, *11*, 440–467.

JM801142B